Aquivion® PFSA-based spray-freeze dried composite materials with SiO$_2$ and TiO$_2$ as hybrid catalysts for the gas phase dehydration of ethanol to ethylene in mild conditions.

Martina Battisti [a,e], Sara Andreoli [a], Riccardo Bacile [a], Claudio Oldani [b], Simona Ortelli [c], Anna Luisa Costa [c], Giuseppe Fornasari [a,d,*], Stefania Albonetti [a,c,*]

[a] Department of Industrial Chemistry "Toso Montanari", University of Bologna, Bologna 40136, Italy
[b] Solvay Specialty Polymers Spa, R&D Centre, Bollate, Milano 20021, Italy
[c] ISTEC-CNR, Institute of Science and Technology for Ceramics, National Research Council, Via Granarolo 64, Faenza 48018, Italy
[d] INSTM, Via G. Giusti, 9, 50121 Firenze, Italy
[e] Chair of Heterogeneous Catalysis and Chemical Technology, ITMC, RWTH Aachen University, Worringerweg 2, 52074 Aachen, Germany

ARTICLE INFO

ABSTRACT

Aquivion PFSA resin, a perfluorinated ion-exchange polymer, has been used as a heterogeneous strong acid catalyst for a range of reactions; however, the activity of this material is limited due to the extremely low surface area of the polymer. In this paper we described the one-step synthesis of Aquivion® PFSA-based hybrid materials using heterocoagulation and spray-freeze-drying of sols containing the precursor of the active phases. The intimated encapsulation of different nano-oxides, such as TiO$_2$ and SiO$_2$ in the superacid resin matrix was easily obtained using this technique and compared with similar catalysts prepared by the impregnation conventional route. The approach led to the preparation of porous micro-granules characterised by a high homogeneity in the phase distribution and high surface area. The prepared materials were active and selective for the gas phase dehydration of ethanol to ethylene in mild conditions. The increase of the porosity improved the activity of the composites, compared to the pure Aquivion® PFSA, and allowed to reduce the amount of the superacid resin. Moreover, the type of encapsulated oxide, TiO$_2$ or SiO$_2$, modified the improved performance of the catalysts, having TiO$_2$ the higher efficiency for ethanol conversion and selectivity in ethylene at very low temperature.

1. Introduction

Ethylene dominates the production of organic compounds in the chemical industry [1] and traditionally, its production relays on the steam-cracking of hydrocarbons [2]. However, to face the depletion of fossil fuels and their impact on the environment, alternative processes are constantly being developed [3–6]. The most promising process for ethylene production is the dehydration of ethanol from bio-sources [7], being the great availability of bioethanol a key factor in the increasing attention towards ethylene production via this path. Many acid catalysts have been put to the test for this reaction: commercial zeolites [8] acid modified aluminas [9] supported 12- tungstophosphoric acid [10,11]. These classes of inorganic catalysts were demonstrated of potentially being able to convert 100% ethanol while producing ethylene. However, ethanol dehydration activities of these catalytic materials were mostly studied at temperatures higher than 300 °C, where the formation of

higher hydrocarbons (> C2) is inevitable [12] and all these catalysts are limited in their industrial application by the reaction temperature required for their use. Therefore, a key factor to increase applicability in a vaster scale could be related to the catalyst's optimization, focusing on lowering the reaction temperature to increase the selectivity, stability and lifespan of the materials [7]. Within this scope, the researchers have been looking for heterogenous catalysts able to provide considerable activity at lower reaction temperatures. Masih et al. have studied small pore RHO type framework zeolites [12] in the temperature range of 200–400 °C. Pd-modified zeolites were the focus of Kamsuwan et al. [13] that investigated the catalytic ethanol dehydration with oxygen cofeeding at 200 °C, demonstrating the importance of increasing the moderate and strong acid sites over the catalysts, while Himmelmann et al. [11] investigated Cs-impregnated silicotungstic acid supported on silicate at 220 °C focusing on by-products selectivity.

Sulfonated acid resins, also known as ion-exchange resins, have been

---

used commercially as heterogeneous acid catalysts able to activate in mild conditions many reactions [14]. Ion-exchange resins family include styrene-based sulfonic materials (Amberlyst® and Dow type resins) which are particularly active in esterification and etherification reactions. Nevertheless, disadvantages of these commercial resins are multiple such as low thermal stability, poor accessibility of active sites, limited mass transfer and excessive swelling in the presence of polar compounds [15] and these properties can limit their application in continuous gas-phase reaction. More recent perflurosulfonic-acid materials, as perfluorosulfonic superacid (PFSA) resin Aquivion® PFSA, have attracted the interest of the scientific community for their unique properties, such as superacidity (Hammett acidity function of −12) and high thermal and chemical stability [16]. Thanks to the perfluorinated structure, Aquivion PFSA shows a high chemical inertness, being adaptable to a variety of reaction and resisting to strong acids, bases and oxidative as well as reductive environments [17–20]. Moreover, Aquivion PFSA displays the shortest side chain compared to its commercially available congeners [21]. This feature increases its crystallinity and raises the glass transition temperature allowing the use at high reaction temperature. Indeed, the perfluorinated structure of this polymer was demonstrated to stand quite high operating temperature without loss in mechanical and chemical integrity [22].

In our previous work [22], the perfluorosulfonic superacid resin- Aquivion® PFSA has been tested in the gas phase dehydration of ethanol at temperatures ranging between 150 and 200 °C. The thermal stability and superacid characteristic of Aquivion® PFSA have been demonstrated to be successful in catalysing the reaction under these mild conditions, reaching conversion up to 90%. However, acid resin activity was demonstrated to strongly depends on the number of accessible acid sites and on material shaping [23,24]. Thus, an optimization of the Aquivion catalyst was necessary to improve the catalytic performance.

The development of a hybrid organic-inorganic composite can overcome these drawbacks by intimately integrating the superacid resin with an inorganic oxide, also reaching the goal to decrease the concentration of expensive PFSA polymer. In the hybrid organic-inorganic materials, the active sulfonated resin is distributed on the surface or in the porous structure of the inorganic support and the presence of a rigid inorganic matrix can prevent the excessive swelling of the resin and at the same time can enhance the accessibility of the active site [2]. Different porous supports have been used to fabricate hybrid materials as zeolites [25], carbon materials [26,27] and clays [28]. In addition, mesoporous silica supports have been extensively studied [29–31].

Various approaches exist for the preparation of hybrid organic-inorganic composites and the catalytic activity is strongly correlated with the efficiency of the method of synthesis. Loading of active phase as a thin layer on porous supports was demonstrated to yield materials with improved accessibility of sulphonic acid sites [32] even though the distribution and homogeneity of polymer coverage of support are challenging goals for this preparation method [2].

An alternative approach to develop a one-step synthesis of organic-inorganic materials with well-controlled compositions and porous textures can be the use of spray technique [33,34]. Spray processed materials have already strongly impacted many sectors such as cosmetics, food and pharmacy. Debecker and co-workers demonstrated the possibility to combinate sol-gel chemistry with aerosol spray drying and this aerosol- assisted process has been proven to be highly effective for the preparation of a wide range of oxide and mixed oxide catalysts [35,36] moreover they demonstrated the possibility to produce using this one-pot method hybrid chemoenzymatic heterogeneous catalysts combining both a stabilized-enzyme and an inorganic catalyst in one bifunctional solid [37,38].

A similar approach with a different process is the use of heterocoagulation and spray-freeze-drying (SFD) of sols containing the precursor of the active phases. This process integrates the colloidal heterocoagulation - exploring the electrostatic self-assembly between the oxide colloidal phase end the Aquivion polymer dispersion - with the aerosol spray management and the evaporation by lyophilization. With this procedure, thermo-labile precursors can be conveniently assembled in colloidal suspensions and dried at low temperatures to produce spherical porous particles and forming high-surface area systems. Using this method, a solvent can be removed without exposing the systems to tensile forces of a receding meniscus [39]. Therefore, it is a suitable drying technique to develop porosity in inorganic and polymeric materials. Moreover, this technique ensures a homogenous incorporation of the active phase into the support, minimizing the possibility of phase separation on a molecular scale [40–42].

In this work polymer/oxide composites (perfluorosulfonic superacid resin- Aquivion® PFSA with SiO_2 and TiO_2) were prepared through heterocoagulation and spray-freeze-drying of sols containing the precursor of the active phases and conventional wet impregnation, for comparison. The aim was to stabilize and increase the porosity of the perfluorosulfonic superacid resin to improve its activity and reduce the Aquivion amount and thus the cost of the catalyst. The SFD method yielded composites with high surface area and homogeneous dispersion of the components. Therefore, the prepared catalysts were tested in the gas phase dehydration of ethanol to ethylene in mild conditions (150–250 °C), to assess the improved performance of these composites compared to the pure Aquivion® PFSA.

2. Experimental

2.1. Materials

The composites were produced at different compositions using a colloidal heterocoagulation method associated with the spray-freeze drying. Titanium dioxide nanopowders (Aeroxide®P25, Evonik mean diameter ≈ 21 nm), silica nanosol (Ludox HS-40, Grace Davison, mean diameter ≈ 12 nm) and Aquivion® PFSA dispersion (Solvay Specialty Polymers, Acid loading 1.28 mmol/g, 25% in water), represent the main components combined to build up the materials. LUDOX® HS-40 is an alkaline, 40% solids, dispersion of silica with a particle size of 12 nm. The silica particles in this grade of colloidal silica are rich in silanol functional groups and carry a negative charge that is stabilized with sodium. The large surface area and surface functionality of LUDOX® HS-40 particles make them an effective binder of metals, oxides, siliceous materials, and polymers with reactive functional groups [43]. For comparison, samples of similar composition were prepared by conventional wet impregnation.

Aquivion® PFSA polymer[44]
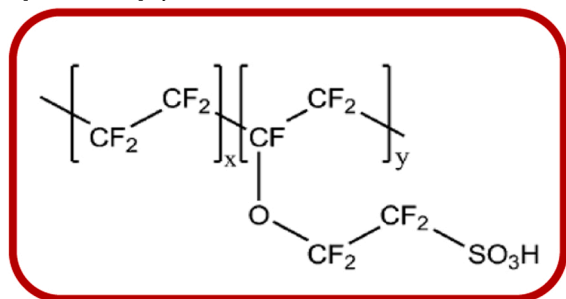
Ludox HS-40
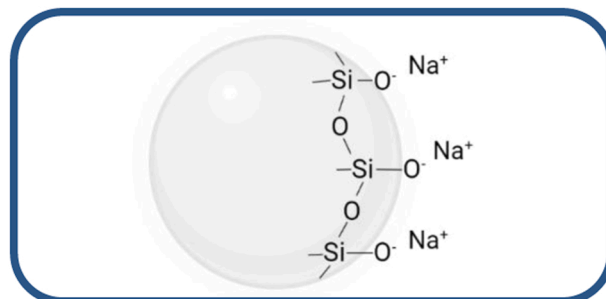
2.1.1. Colloidal preparation

The Multicomponent Aquivion/SiO₂ and Aquivion/TiO₂ samples have been obtained by means of a heterocoagulation colloidal process and then granulated to achieve a micrometric highly reactive porous powder. In order to better evaluate the influence of SiO₂ and TiO₂ on the activity, different Aquivion/oxides mass ratios have been investigated, preparing the samples listed in Table 1.

To carry out the heterocoagulation process, the commercial SiO₂ nanosol, (Ludox HS40 pH = 9) was subjected to a resin treatment, by means of a cationic exchange resin (DOWEX 50 ×8) to eliminate Na⁺ and decrease pH. As a matter of fact, the basic original pH of the SiO₂ nanosol Ludox HS40 could prevent the coupling with acidic Aquivion, due to very likely instantaneous flocculation, moreover the elimination of Na⁺, can activate the reactive functionality present on SiO₂ nanoparticles surface favouring network formation. Therefore, the pH of colloidal silica was decreased to 4 by resin treatment. After appropriate dilution in water to 25 wt%, the silica nanosol was slowly dripped, under stirring, in Aquivion_sol at the concentration of 12.5 wt%. Aquivion/TiO₂ samples were prepared in a similar way. Titania P25 powder was suspended in acidic water (in HCl at pH = 3.5) at the concentration of 25 wt%. The two phases were mixed by dripping under stirring of TiO₂ P25 nanosol in Aquivion_sol at the concentration of 12.5 wt%. The mixtures were ball-milled for 24 h using ZrO₂ grinding media (5 nm diameter size). Different amount of the two phases, metal oxides (SiO₂ and TiO₂) and Aquivion, were mixed for obtaining the different Aquivion/metal oxide ratios (Aquivion 20%, 30% and 40%). The multicomponent Aquivion/SiO₂ and Aquivion/TiO₂ samples were prepared at final total concentration of 20 wt% to ensure good processability during following spray freeze granulation step.

2.1.2. Spray freeze granulation process

The spray-freeze-granulation technique (Fig. S1) has been here employed to obtain micrometric powders, starting from biphasic Aquivion/metal oxide nanosols, by means of the lab-scale granulator instrument, LS-2. The mixed suspensions were atomized through a peristaltic pump, blowing nitrogen gas at 0.4 bar through a 100 μm nozzle and nebulized into a stirred solution of liquid nitrogen, to enable an instantaneous freezing of each generated drop. The so-frozen drops were placed into a freeze-drying apparatus with a pressure of 0.15 mbar and a temperature of − 1 °C, to promote the sublimation process, which

was completed within 48 h, and producing a highly porous granulated powder. Part of the catalysts has undergone a calcination treatment at 300 °C (2 h of residence time and a heating velocity of 100 °C/h) aimed to consolidate the granule structure.

2.1.3. Preparation of catalysts using wet impregnation

The wet impregnated samples were prepared using titanium dioxide nanopowders (Aeroxide®P25, Evonik mean diameter ≈ 21 nm) and silica (Davicat 1403, Grace Davison) as supports and Aquivion® PFSA dispersion (D65, Solvay Specialty Polymers) in different amounts as active phase. The prepared catalysts were dried first in a rotavapor and in air at 150 °C overnight and then calcined in air at 300 °C for 3 h.

The samples prepared following this technique are labelled as W to be distinguished from those prepared after the spray-freeze drying treatment and reported in Table 1.

2.2. Characterization

2.2.1. Analytical characterization

Zeta potential measurements on the colloidal samples were performed at 25 °C by Electrophoretic Light Scattering (ELS) technique by means of the instrument Zetasizer nano ZSP (Malvern Instruments, UK). Smoluchowski equation was applied to convert the electrophoretic mobility to zeta potential. After a 2 min temperature equilibration step, samples underwent three measurements, and zeta potential was obtained by averaging these measurements. The instrument is equipped with an auto-titration unit enabling the identification of the isoelectric point (pH_{IEP}) and adding automatically to the sample KOH 0.1 M or HCl 0.1 M, in order to explore the Zeta potential trend within a selected pH range. The measurements were performed on different samples (Aquivion and metal oxides - SiO₂ and TiO₂ - singularly and in mixtures) diluted 1:100 with distilled water.

The granulated catalysts were observed by scanning electronic microscopy using a Field Emission Scanning Electron Microscope, FESEM (Carl Zeiss Sigma NTS, Germany). The granules were fixed to aluminium stubs with conductive adhesive tape. Elemental analysis was performed by image analysis using FESEM coupled to an energy dispersive X-ray micro-analyzer (EDS, mod. INCA).

XRD measurements were carried out at room temperature with a Bragg/Brentano diffractometer (X′pertPro PANalytical) equipped with a fast X′Celerator detector, using a Cu anode as the X-ray source (Kα, λ = 1.5418 Å). Diffractograms were recorded in the range 5–80° 2θ counting for 15 s every 0.05° 2θ step.

Thermal behaviour of Aquivion® PFSA was followed through thermogravimetric analysis performed in a TA Instrument Q600. The analysis was performed by heating the powder samples from RT to 800 °C, 10 °C/min under air flow and then kept at 800 °C for 5 min.

The textural properties of the samples were measured from N2 adsorption-desorption isotherms at 77 K on a Micromeritics ASAP 2020 surface area analyser. Samples were previously outgassed for 30 min at 150 °C and 15 μmHg, and then held for 30 min at 240 °C. Specific surface area values were obtained by multi-point BET equation while average diameter of the pores and pore volumes using BJH method.

2.3. Catalytic tests

The catalytic behaviour of Aquivion composites was investigated in the gas-phase dehydration of ethanol to ethylene as reported elsewhere [22]. The catalytic tests were carried out in a laboratory scale plant equipped with a syringe pump for ethanol feeding, gas flow meters and a glass fixed-bed down-flow reactor. The catalyst was placed in the isothermal area of the reactor on a fritted glass plate. The catalysts performance was determined at atmospheric pressure and at temperature in the range from 150° to 250 °C with a feeding stream of 1% v/v of ethanol in helium. The reaction products were detected on-line with a TCD-gas-cromatograph apparatus equipped with a CP-Sil 5 CB column

Table 1

Structural parameters, chemical composition and acidity of the Aquivion/SiO₂ and Aquivion/TiO₂ prepared catalysts. WET: wet impregnation; SFD: spray-freeze-drying.

Sample	Theoretical Aquivion content [%]	Experimental Aquivion content [%]*	SA$_{BET}$ [m²/g]	Acidity [mmol/g$_{cat}$]*	Preparation
Aquivion® PFSA	100	100	0	1.28	Commercial
SiO₂ SFD	0	0	220	0	SFD
Aq-SiO₂-20	20	18	116	0.23	SFD
Aq-SiO₂-30	30	28	75	0.37	SFD
Aq-SiO₂-40	40	46	34	0.55	SFD
SiO₂	0	0	260	0	Commercial
Aq-SiO₂-20 W	20	18	206	0.23	WET
Aq-SiO₂-30 W	30	34	140	0.43	WET
Aq-SiO₂-40 W	40	44	10	0.56	WET
TiO₂	0	0	50	0	Commercial
Aq-TiO₂-20	20	20	26	0.26	SFD
Aq-TiO₂-30	30	39	11	0.50	SFD
Aq-TiO₂-40	40	50	10	0.64	SFD
Aq-TiO₂-40 W	40	52	4	0.66	WET

* Estimated by weight loss in TG analyses

(30 m x 0.53 mm × 0.70 mm) maintained at 40 °C during the analysis. The catalysts were stabilized at 150 °C for 1 h under nitrogen flow before each test, in order to remove the moisture from Aquivion surface. Calculated carbon balances, if not differently indicated, were 95 ± 5%.

3. Results and discussion

3.1. Colloidal and morphological characterization of Aquivion® PFSA based catalysts prepared using Spray-Freeze-Drying

The multicomponent Aquivion/SiO$_2$ and Aquivion/TiO$_2$ composites were produced at different compositions using a colloidal hetero-coagulation method, expected to give rise to "matrix encapsulation" [45], associated with the spray-freeze drying. Using a colloidal approach, the best conditions driving the self-assembled hetero-coagulation process between different colloidal phases coincide with the species exhibiting ζ -potentials, at the working pH, that are opposite in sign and high enough to ensure colloidal stabilization and avoid homocoagulation. In the present case, however, it proved necessary to decrease the colloidal stabilization of the silica by reducing its pH in order to promote the polymer's coagulation over the SiO$_2$ or TiO$_2$ nano surfaces (heterocoagulation). However, pristine SiO$_2$ nanoparticles (NPs) and Aquivion® PFSA were both negatively charged (Fig. 1a) but the resin-modified silica showed a significant decrease in ζ-potential suggesting a reorganization of the SiO$_2$ with a perfluorosulfonic super-acid resin shell, which could indicate that polymer encapsulated structures are obtained (drawing in Fig. 1). A more compact structure was expected from Aquivion/TiO$_2$ composite if compared with Aquivion/SiO$_2$, due to strong electrostatic interactions between positively charged TiO$_2$ NPs and negatively charged polymer at working pH= 4 (Fig. 1b). The high correspondence found in NPs-polymer composites (NPs/polymer – grey) and Aquivion® PFSA polymer (blue) curves suggested the covering of NPs by the polymer.

The so-obtained sols were processed by spray-freeze drying (Fig. S1), exploiting the instantaneous the freezing of the spray droplets containing the nano-oxide and the polymeric latex, intimately mixed. This allowed, after the sublimation process, the preservation of nano-structure and forming a stable network, in the SFD granules [40–42]. Moreover, the free silanol groups, present on nano oxide surface, should help in matrix encapsulation of sulfonic resins.

The FESEM micrographs of both samples (Fig. 2) reveals a primary structure that is very fine, as demonstrated by the high magnification image, but organized in the form of micrometric diffused aggregates, as shown by Fig. 2a and Fig. 2b for Aq-SiO$_2$-40 and Aq-TiO$_2$-40,

respectively. The dispersion of the different components was very homogeneous in all the studied systems as also observed in other composites prepared by the coupling of heterocoagulation and SFD processes [35]. This was further demonstrated by SEM-EDX analysis. Fig. 3 reports the chemical composition of the different composites investigated by EDX. Fig. 3a displays a very homogeneous distribution of the different species (Si, F and S) without any apparent segregation in Aq-SiO$_2$-40 sample obtained by SFD. Otherwise, the sample Aq-SiO$_2$-40 W sample obtained by wet impregnation (Fig. 3b) shows a certain inhomogeneity particularly evident for the S and F elements.

The as synthesized and calcined catalysts were lightweight flowable powders with high specific surface area, reduced as a function of the loading of the polymer (Table 1). It is reasonable to hypothesize that the composites which showed a drastic drop in SSA are the result of a more intimate blending with the polymer as further confirmed by the over-lapping of Zeta pot vs pH curves of polymer and composite at the highest concentration of polymer (Fig. 1). This effect is more pronounced using high surface area silica powder as a support for wet impregnation of Aquivion, where the polymer resulted less homogeneously dispersed. However, the importance of the spray freeze-drying process stays on the possibility of increasing the dispersion and intimate contact of Aquivion with nano-oxide. This is due to the homogenous molecular incorporation of the active phase into the inorganic support at liquid state, which minimize the possibility of phase separation.

3.2. Characterization of Aquivion/SiO$_2$ composites

The thermal degradation of the composite materials was analysed through thermogravimetric (TG) analysis in air. This method was used to verify the decomposition trend of different hybrid organic-inorganic materials and the effective Aquivion loading of the different catalysts reported in Table 1.

Bare Aquivion sulfonic resin is known to start decomposing at 280 °C, temperature which leads to the desulphonation process. Then, the PFSA loses the side chains starting from a temperature of around 360 °C, and finally the perfluorocarbon backbone starts decomposing at around 400 °C [22]. These three decomposition steps are visible in the TGA profiles associated with pure Aquivion that are reported in Fig. S2 and Fig. S3.

The different silica containing composites present a higher decomposition temperature than the one of pure Aquivion, this behaviour is evidenced by the shifting at higher temperature of the TGA curve and it is particularly evident for sample with a low load of active phase (20% Aquivion). Indeed, increasing the load of Aquivion, the decomposition
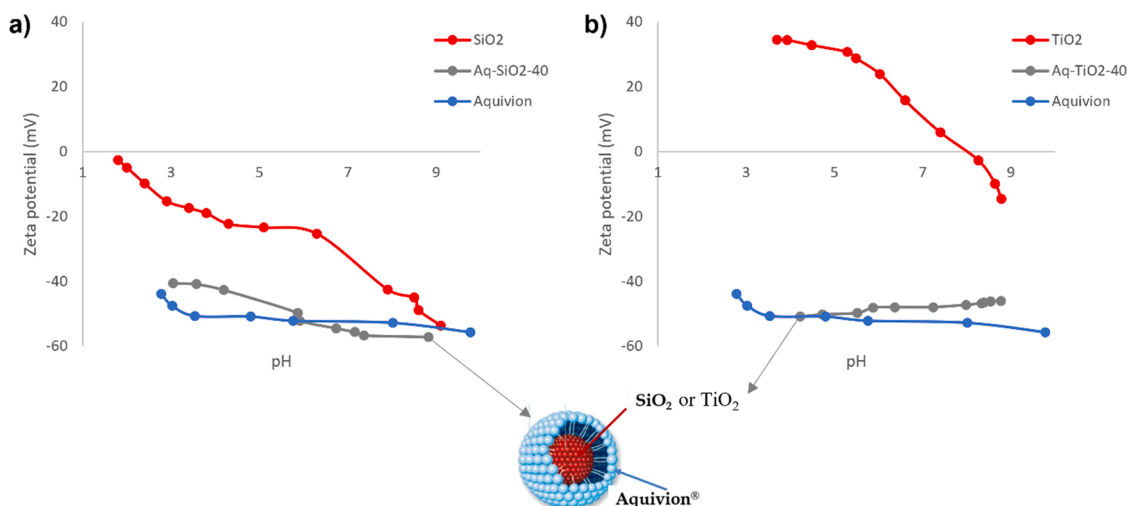

Fig. 1. Zeta potential as a function of pH for (a) SiO$_2$, Aquivion and Aq-SiO$_2$-40 mixture; (b) TiO$_2$, Aquivion and Aq-TiO$_2$-40 mixture.
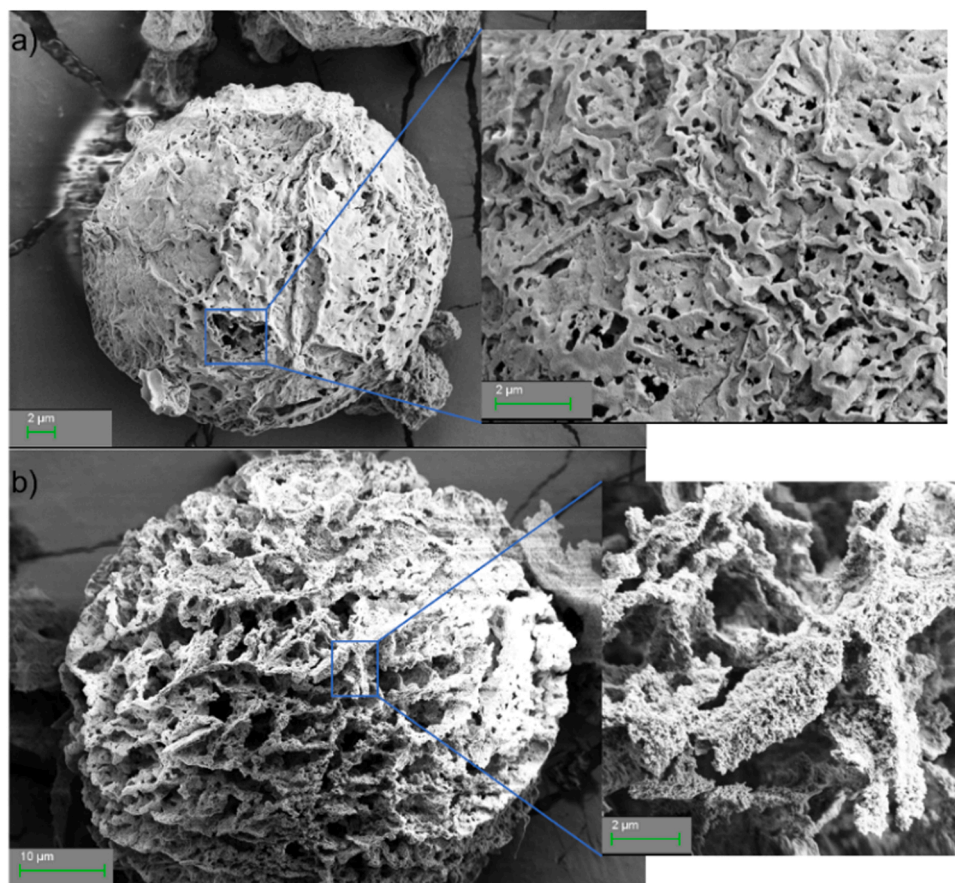
Fig. 2. FESEM images of SFD powders from (a) Aquivion-SiO$_2$ sol and (b) Aquivion-TiO$_2$ sol.

temperature of the supported sample decreases both in supported (Fig. S2) and SFD (Fig. S3) samples becoming closer to the one of pure Aquivion. These results agree with previous studies [30].

Since the SiO$_2$ support is not decomposed in the temperature range of the TG analysis (25–800 °C), the weight loss experienced by the sample can be only attributed to the decomposition of Aquivion. Consequently, it is possible to verify the effective weight of Aquivion in the catalyst reported in Table 1. The Aquivion/SiO$_2$ samples present an effective weight loss which is very similar to the theoretical Aquivion content. The slight differences can be attributed at the experimental error during the procedure. Nonetheless, the results demonstrate that both the WET synthetical method and the SDF are simple and reliable option to produce catalysts with the desired active phase load.

The XRD analysis has been used to investigate the crystalline phases present in the Aquivion/SiO$_2$ catalysts after calcination at 300 °C. The samples prepared through SFD, reported in Fig. 4, show the typical spectrum of amorphous SiO$_2$, with the broad band around 23° 2θ [46, 47] and the reflects of pure Aquivion, characterised by two bands associated with the perfluorocarbon backbone of the polymer. The asymmetrical band at approximately 18° 2θ is composed of a wide band at 17.2° 2θ representing the scattering of the amorphous phase and a narrow band at 18.2° 2θ representing the diffraction of the crystalline phase [48]. The band is linked to the distance between two polytetrafluoroethylene segments, while the broad band centred at around 40° 2θ is attributed to the distance between CF$_2$ groups [16,49]. The composite materials generally present an overlap of the characteristic diffractograms of both Aquivion and SiO$_2$, with the Aquivion reflects becoming more visible as its load increase. The effect of calcination is not significantly evident from these data and the obtained results confirm the integrity of the resins after thermal treatment in air at T = 300 °C. The same trend observed for the SFD composites is followed by the WET

samples (Fig. S4).

The acidity of Aquivion resins can directly be analysed by acid-base potentiometric titrations as reported elsewhere [30], nevertheless repeated measurement on our hybrid materials yielded a significant irreproducibility not allowing the use of these data for catalysts comparison. Moreover, repeated attempt to perform a quantitative determination of acid sites on the prepared catalysts with reliable spectroscopic approaches and calorimetry using basic probe molecules were for the moment unsuccessful. Since solid state ^{13}C NMR MAS and ^{19}F NMR MAS confirmed the structural integrity of the Aquivion resin after thermal treatment (Fig. S5), an estimation of acid sites in different samples were indirectly deduced from TG analysis (Table 1) using the Aquivion content and the Acid loading of 1.28 mmol/g. Dou et al. [32] demonstrated that these data are well correlated to the density of acid sites determined by other techniques for hybrid materials at low Aquivion loading. Nevertheless, with increasing Aquivion loading other methods has to be implemented and a series of NMR – MAS analysis with probe molecules are in progress for these composites.

The porosity of series Aquivion/SiO$_2$ composites were characterized by N$_2$ physisorption.

All the prepared catalysts display a type IV isotherm pattern (Table 2 and Fig. S6-S9). The hysteresis loop observed at a relative pressure between 0.4 and 0.9 is typical of a mesoporous structure, the external surface area values determined by t-plot analysis show that microporosity is not present. The increase of the Aquivion amount decreases the surface area and the pore volume, due to the intimate blending with the polymer (covering, pore filling, pore blocking, etc.). The average diameter of the pores of the material undergoes a marked increase, suggesting that the polymer blocks or fills the fine porosities of the composite. For the sample prepared by impregnation the porous structure of the silica is occupied by the polymer and the decrease of surface
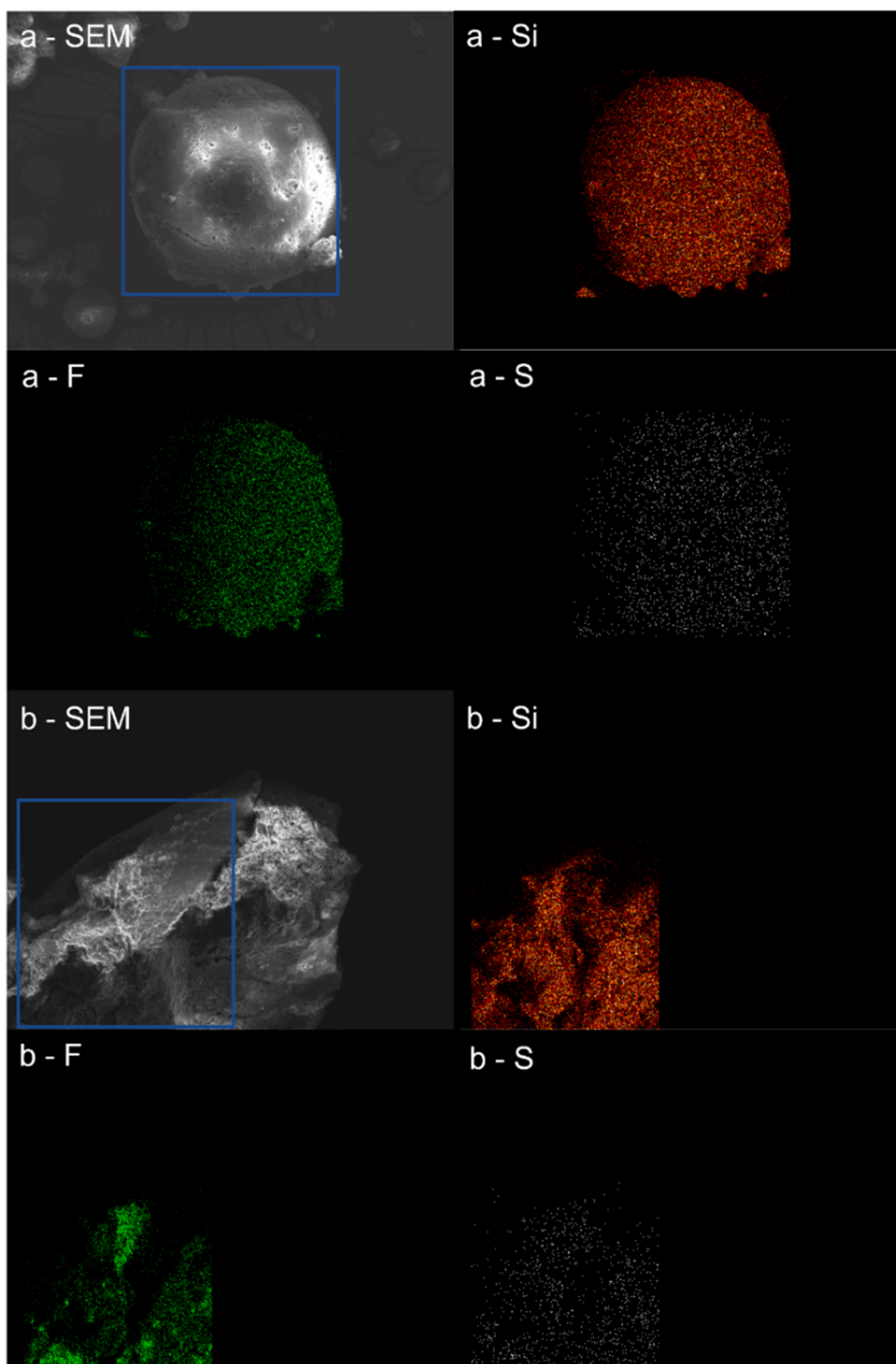
Fig. 3. SEM-EDX maps of the samples Aq-SiO$_2$-40 SFD (a) and Aq-SiO$_2$-40 W (b). SEM images, Si maps (red), F maps (green) and S maps (white).

area and pore volume is even more evident.

3.3. Characterization of Aquivion/TiO$_2$ composites

Similarly, to what has been done with Aq-SiO$_2$ composites, the thermal properties and effective active phase load for Aq-TiO$_2$ samples was assessed using TG analysis. The thermograms for the TiO$_2$-incorporated samples are reported in Fig. S10, while Table 1 reports the weight loss percentages experienced during the TG analyses.

Differently to what happens with SiO$_2$, the immobilization of Aquivion over TiO$_2$ does not positively impacts the decomposition temperature of the catalyst. Indeed, the Aquivion/TiO$_2$ catalysts start decomposing at the same temperature of pure Aquivion, regardless of the synthetical method or the Aquivion content. Therefore, it appears that titania does not provide the same thermal stabilization to the PFSA observed with silica. The weight loss percentages reported in Table 1 highlight that, while the sample with 20% Aquivion load presents an experimental content equal to the theoretical one, the catalysts with a higher load of Aquivion display a gap between the two percentages. Regardless of the synthesis method (WET or SFD), the samples show an experimental content of Aquivion around 10% points higher than the expected one.
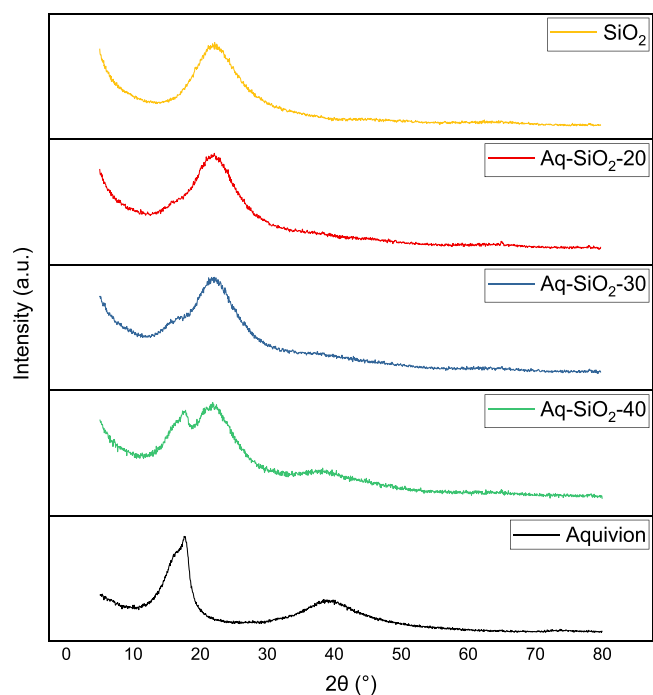
Fig. 4. XRD patterns of SiO₂, Aquivion and Aquivion/SiO₂ composites synthesized by SFD and calcined at 300 °C.

Table 2
Textural property of Aquivion based catalysts.

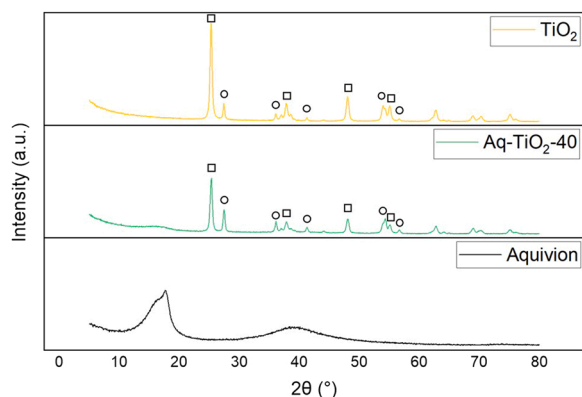| Sample	SA_{BET} [m²/g]	External SA (m²/g)	Dpore (nm)*	Vpore (cm³g⁻¹)*
Aquivion® PFSA	0	-	-	0
SiO₂ SFD	220	-		
Aq-SiO₂-20	116	115	6	0,22
Aq-SiO2–30	75	76	7	0,17
Aq-SiO₂-40	34	35	11	0,12
Aq-SiO₂-40 W	10	10	35	0,09
TiO2-P25	50	50	15	0,19
Aq-TiO₂-20	26	25	18	0,16
Aq-TiO₂-30	11	12	27	0,09
Aq-TiO₂-40	10	10	26	0,07
Aq-TiO₂-40 W	4	4	15	0,02

* Calculated by BJH method

Fig. 5. XRD patterns of TiO₂ (Commercial P25), Aquivion and Aquivion/TiO₂ composites synthesized by SFD and calcined at 300 °C. □ = Anatase; ○ = Rutile.

The considerations for the XRD analysis for the Aquivion/TiO₂ catalysts calcined at 300 °C (Fig. 5) are analogous to the previously discussed Aquivion/SiO₂ ones. The diffractogram of commercial TiO₂ presents the characteristic reflects associated with P25 TiO₂ powder consisting of 80% Anatase and 20% Rutile. The addition of Aquivion over the inorganic matrix is highlighted by the presence of the two broad peaks associated with its perfluorocarbon backbone. For the sake of simplicity, only the diffractogram of Aq-TiO₂-40 is reported, since the same considerations can be drawn for the other samples.

The porosity of series Aquivion/TiO₂ composites were characterized by N₂ physisorption.

All the prepared catalysts display a Type IV isotherm pattern (Table 2 and Fig. S11-S14) with the hysteresis loop observed at a relative pressure higher than 0.75. The materials show a mesoporous structure with a higher average diameter of the pores and a lower surface area than those of Aquivion/SiO₂. Also, in this case the increase of the Aquivion amount decreases the surface area and the pore volume. The bare TiO₂ P25 does not contain pores in the crystallites. The formation of porous structure can be attributed to the aggregations of TiO₂ crystallites. The average pore diameter coincides with the TiO2 crystallite size [50]. The TiO₂ P25 has a surface area of 50 m²/g and a mean pore diameter of 15 nm like those reported in literature. The surface area and pore volume of the WET sample prepared by impregnation are very low and it appears that the porous structure formed of the aggregates of TiO₂ crystallites is covered by the polymer.

3.4. Catalytic activity

The Aquivion-SiO₂ and Aquivion-TiO₂ samples were tested as heterogeneous catalysts in the continuous gas-phase process for the dehydration of ethanol in mild conditions. In this reaction (Scheme 1), the main detected products were ethylene and diethyl ether (DEE). The DEE formation proceeds through a condensation reaction between two ethanol molecules (Reaction 2), an exothermic process disfavoured by increasing temperatures. The main controversy lies in the production of ethylene, which can derive from direct ethanol dehydration (Reaction 1), from the decomposition of the DEE (Reaction 3), or from the coexistence of both routes [2,51].

In a previous article from the research group, the ethanol dehydration was studied using pure Aquivion as heterogeneous catalyst [22]. Aquivion showed very high ethanol conversion and ethylene selectivity, remaining stable during 14 h on stream. However, its use was penalised by the low accessibility of acid sites in the gas phase. Indeed, being a gel-type resin, the majority of the sulfonic acid sites of Aquivion-based catalysts are expected to be buried within the polymer, leading to the reactants reduced accessibility to the active sites [52]. The reactivity of the catalyst is negatively influenced also by the consequent low surface area, which further complicates mass transfer. To increase the porosity, Aquivion/SiO₂ and Aquivion/TiO₂ catalysts have been synthesised using heterocoagulation and spray-freeze-drying (SFD) of sols
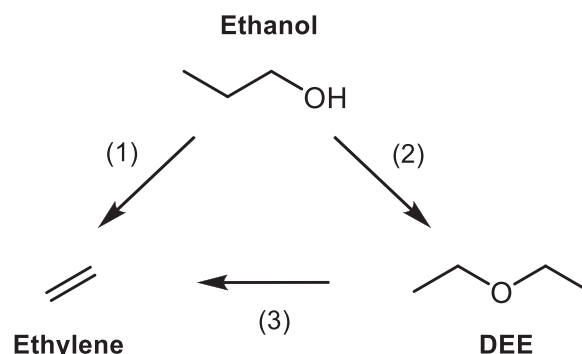
Scheme 1. Ethanol dehydration to ethylene and diethyl ether (DEE).

containing the precursor of the active phases and conventional wet impregnation, for comparison.

3.4.1. Aquivion® PFSA based catalysts prepared using SiO$_2$

Firstly, the use of the sole silica with a high surface area has been investigated for the dehydration of ethanol, to assess its catalytic contribute to the reaction. The trend for EtOH conversion and ethylene yield at increasing temperatures (150–250 °C) is reported in Fig. S15. Silica has no catalytic activity, since ethanol conversion is negligible (< 2%) under all the temperatures analysed. With silica, the only product observed is ethylene, with yields lower than 2%, according to the need for the reaction of a low acid strength, while DEE is not formed at any temperature.

3.4.1.1. Study of the catalytic activity of Aquivion/SiO$_2$ catalysts synthesised via Wet impregnation.
Aquivion/SiO$_2$ catalysts synthesised via wet impregnation with different Aquivion loads (20, 30 and 40 wt%) were used for studying their activity for ethanol dehydration to produce ethylene. The measurements of the catalytic activities were always performed as a function of time and temperatures for the different materials. Since ethanol conversion and products yields were quite stable after 90 min of reaction (see as an example Fig. S16 summarizing the data for sample Aq-SiO2–40w**)**, the catalytic results compared in the manuscript graphs resulted from the averaged of measurements taken for an hour of reaction after stabilization.

Fig. 6 **shows** the influence of different temperatures (150–200–250 °C) over the catalytic activity assessed for Aq-SiO$_2$-20 W (Aquivion load: 20 wt%). Increasing temperatures are associated with a trend in conversion and yield. As a general observation, increasing temperatures leads to higher ethanol conversions, from 25% to 56%. The same trend is reflected in ethylene selectivity, which grows from 17% to 86%. The effect of temperature over selectivity is consistent with the work of Knözinger et al. [53]. The formation of DEE from ethanol is favoured at low temperatures and low conversions, being the reaction bimolecular and with a high reaction order. Under these conditions, ethylene production is likely to proceed via ether decomposition and cracking (Reaction 3). On the contrary, with increasing temperatures, ethylene formation mainly occurs through direct dehydration of ethanol, becoming the only reaction at temperatures higher than 225 °C.
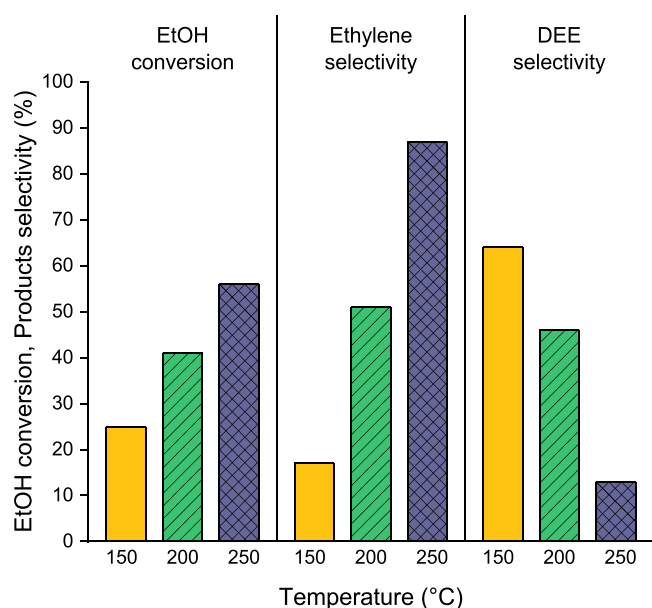
In addition to the main products, the ethanol dehydration can also generate negligible amount of by-products that will not be considered, such acetaldehyde, whose production is believed to happen above 300°.

Thus, in our tests, at 150 °C the formation of DEE over ethylene is facilitated, with a higher selectivity for DEE (64%) compared to the 17% value obtained for ethylene. This trend inverts from 200 °C and above, where ethylene becomes the principal product, and DEE formation is disfavoured (13% selectivity at 250 °C). DEE formation derives from intermolecular condensation of ethanol and is favoured at low temperatures. Conversely, ethylene derives from ethanol intramolecular dehydration, an endothermic reaction, and thus favoured at high temperatures. Even though conversion and ethylene selectivity values are considerable at 250 °C, none of the conditions analysed allow to convert the totality of ethanol.

Another important parameter for the reaction is the catalyst load of Aquivion. A set of experiments with three different amounts of Aquivion – 20, 30 and 40 wt% – was performed to study the effect of active phase load supported on silica. The tests were performed at 200 °C and atmospheric pressure, with a contact time τ of 1 s and a 1%(v/v) EtOH flux in He. The catalysts used were Aq-SiO$_2$-20 W, Aq-SiO$_2$-30 W and Aq-SiO$_2$-40 W with 20, 30 and 40 wt% Aquivion loads, respectively.

Fig. 7 shows ethanol conversion and products selectivity versus the Aquivion load of the impregnated SiO$_2$ catalyst. When the Aquivion content was increased from 20 wt% to 30 wt% and then further to 40 wt %, the conversion of EtOH at 200 °C increases from 41% to 80% and then stabilizes (81%). The same trend is reflected in the ethylene selectivity, which goes from 51% to 64% and then remains approximately stable (67%) even if the Aquivion content increases. On the other hand, the data show an opposite tendency of DEE selectivity, which slightly decreases from 19% to 14% with growing Aquivion loads. As data suggest, the activity improvement is more significative going from 20 to 30 wt% of Aquivion load in the catalyst, rather than increasing the percentage of active phase up to 40 wt%.

A possible explanation for this behaviour was suggested by Bringue et al. [54] in their study of supported Nafion catalysts for 1-penthanol dehydration. As the percentage of active phase supported on the carrier increases, the catalytic activity increases, until it reaches an optimum. This happens when the whole accessible surface of the support is covered with Nafion or Aquivion, thus all the active sites are perfectly distributed and accessible. At higher percentages, the
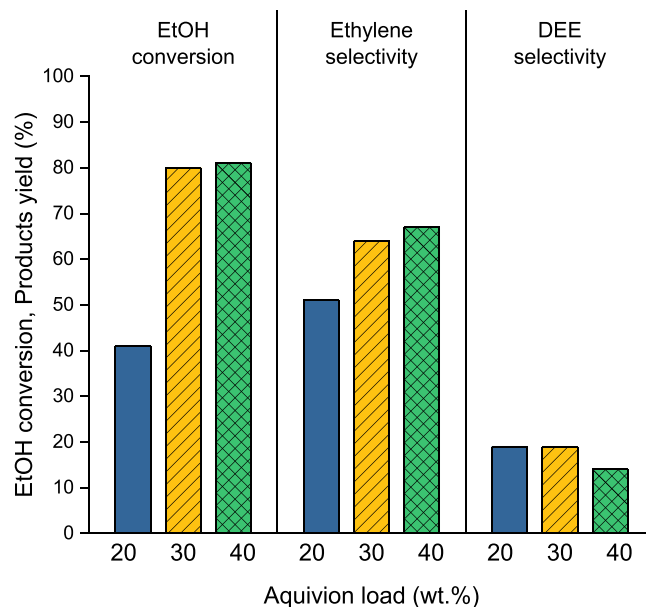

Fig. 6. Trend of the catalytic activity of **Aq-SiO$_2$-20 W**, prepared by wet impregnation, with temperature (T = 150–200–250 °C). Test conditions: m_{cat} = 0,24 g, τ = 1 s, EtOH = 1% v/v.

Fig. 7. Influence of the Aquivion load: 20, 30 or 40% over wet impregnated Aquivion/SiO$_2$ catalysts. Test conditions: T = 200 °C, τ = 1 s, EtOH = 1% v/v,.

perfluorosulphonic acid polymers start to bond to other polymer chains, blocking some pores and reducing the accessibility to the inner active centres. The consequence is the decrease of the turnover number, which is reflected in the plateau of the catalytic activity with 40 wt% Aquivion load.

3.4.1.2. Study of the catalytic activity of Aquivion/SiO₂ catalysts synthetised via Spray-Freeze-Drying. The Aquivion/SiO₂ composite catalysts prepared via Spray-Freeze-Drying (SFD) were applied in the ethanol dehydration reaction, analogously to the ones synthesised through wet impregnation. At first the catalytic activity was assessed progressively increasing the reaction temperature from 150° to 250°C, to evaluate the catalytic performance and the optimal conditions to carry out the following activity tests. This temperature screening was performed with Aq-SiO₂-30 (30 wt% of Aquivion), with a contact time of 1 s, and feeding 1% (v/v) EtOH in He. The results are reported in Fig. S17. As already observed for impregnated catalysts, EtOH conversion and ethylene selectivity are positively influenced by a temperature increase, reaching a 94% conversion and an 80% ethylene selectivity at 250 °C. Conversely, selectivity for DEE decreases with higher temperatures, since the intermolecular condensation of ethanol is an exothermic reaction, reaching negligible values (1%) at 250 °C. Indeed, at low temperatures (150 °C), DEE production is favoured over ethylene formation (selectivity: 50% for DEE vs 24% for ethylene). When the temperature goes up to 200 °C, ethylene production is promoted since it can happen both through dehydration of EtOH and decomposition of DEE. Thus, ethylene becomes the principal product, with higher selectivity while DEE is only present as a by-product.

It is then possible to compare Aquivion/SiO₂ catalysts prepared using SFD with different loads of Aquivion (Aq-SiO₂-20, Aq-SiO₂-30 and Aq-SiO₂-40, respectively with 20, 30 and 40 wt% Aquivion load), as previously done with impregnated samples. Fig. 8 shows the performance of these catalysts in ethanol dehydration, investigated at 200 °C, with a contact time τ of 1 s and a 1%(v/v) EtOH flux in He. As the data demonstrate, the catalyst with the intermediate active phase load (30 wt%) shows the optimal catalytic activity, reaching 89% ethanol conversion, a selectivity for ethylene of 73% and only a DEE selectivity of 9%. On the other hand, Aq-SiO₂-40 presents an intermediate activity, which can be linked to its surface area. The BET data highlight that the SFD catalysts have lower surface area values compared to impregnated catalysts. A high load of active phase combined with a low surface area
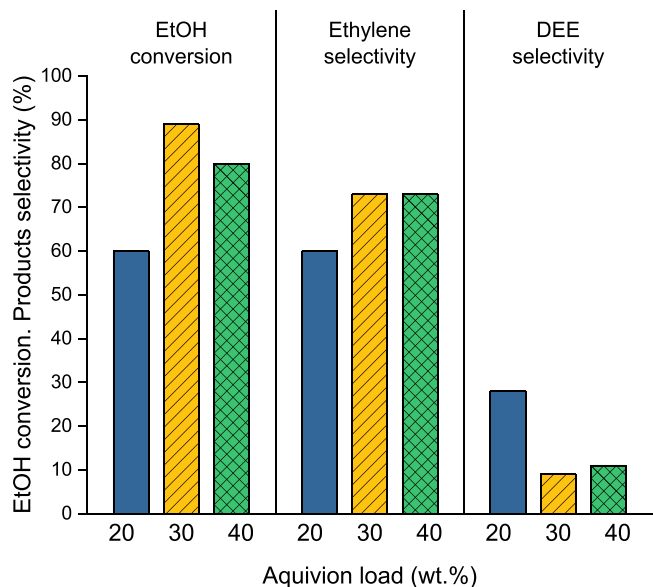
leads to the obstruction of the silica pores, with the following reduction of catalytic activity of the catalyst. These results confirmed previous studies that showed the presence of an optimum load of polymer maximizing catalytic activity [48].

At this point, the two different synthetical methods can be compared to appreciate any difference in the catalytic activity. The conversion and selectivity values reported in Fig. 9 refer to Aq-SiO₂-20 W and Aq-SiO₂-20. The two catalysts both present a 20 wt% load of Aquivion and were respectively prepared via wet impregnation and spray-freeze-drying. The SFD sample clearly shows superior catalytic activity than the WET one. Indeed, under the same reaction conditions, the EtOH conversion goes from 41% to 60%, with a higher ethylene production since the selectivity value increases from 51% to 60%. Additionally, a considerable reduction in DEE selectivity is observed, from 46% with the WET catalyst to 28% with the SFD sample. These trends are also confirmed at larger Aquivion content, confirming the superiority of the SFD synthetical method to produce Aquivion composites active in the dehydration of ethanol.

3.4.2. Aquivion® PFSA based catalysts prepared using TiO₂

Other than silica, titania is one of the most studied metal oxides because of its wide range of applications as a support in catalytic and photocatalytic applications, solar cells, and biocompatible implants [55]. Before the application of TiO₂ as a support in the reaction under analysis, its catalytic activity was tested, analogously to what has been done with silica. The data (Fig. S18) show that the sole titania is not an effective catalyst for the dehydration of ethanol, as it presents negligible conversion and yield values. However, when titanium oxide is used as a support for Aquivion, the resulting composite material demonstrates impressive catalytic activity in the reaction under analysis.

In Fig. 10, EtOH conversion and ethylene and DEE selectivities are expressed as a function of the Aquivion load of titania-based catalysts synthetised through SFD. The catalysts under analysis are Aq-TiO₂-20, Aq-TiO₂-30, and Aq-TiO₂-40 respectively with 20, 30 and 40 wt% of Aquivion load. Moreover, the conversion and selectivity obtained with pure Aquivion in a previous study are reported for comparison [22]. The test conditions utilised are a 150 °C temperature, with a 1 s contact time and a 1% (v/v) EtOH feed. With Aq-TiO₂-20, a high conversion value (86%) and ethylene selectivity (72%) are achieved, but at the same time
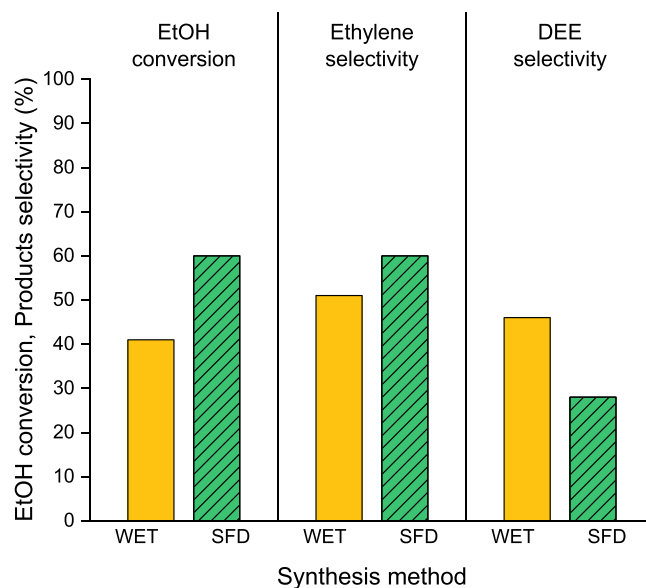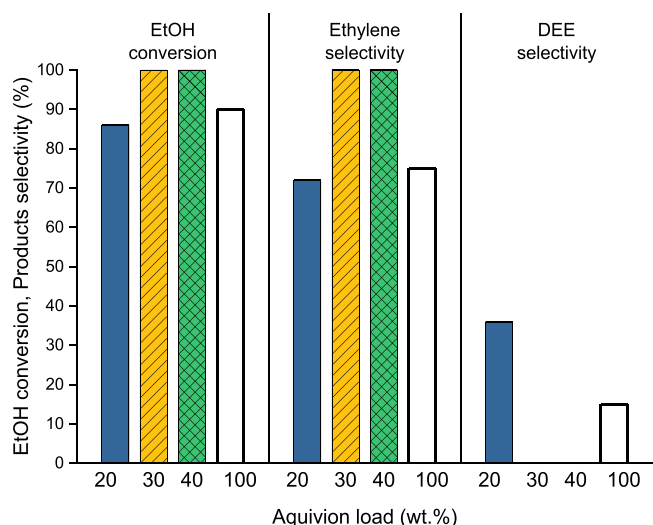

Fig. 8. Influence of the Aquivion load (20, 30 or 40 wt%) over spray freeze drying Aq-SiO₂ catalysts. Test conditions: T = 200 °C, τ = 1 s, EtOH = 1% v/v.

Fig. 9. The dependence of conversion and selectivity on the synthesis method (WET= wet impregnation, SFD= spray freeze drying) using Aq-SiO₂ catalysts with 20 wt% Aquivion load. Test conditions: T = 200°C, τ = 1 s, EtOH = 1% v/v.

Fig. 10. Influence of the Aquivion load (20, 30 or 40 wt%) over spray freeze drying Aquivion/TiO$_2$ catalysts. The white rectangle refers to the Aquivion catalyst (powder) analysed in a previous study [22]. Test conditions: T = 150 °C, τ = 1 s, EtOH = 1% v/v.

a consistent amount of DEE is produced (36% selectivity). Increasing the active phase load to 30 wt% and 40 wt% raised the EtOH conversion and ethylene selectivity up to 100%, while no trace of DEE was found in the exiting stream. When the TiO$_2$-supported catalysts are compared to pure Aquivion, the presence of only 20 wt% of Aquivion over titania showed inferior catalytic activity than the pure one, with slightly minor conversion (86% vs 90%) and ethylene selectivity (72% vs 76%) and a considerably major production of DEE (36% vs 16%). On the contrary, despite the lower quantity of active phase in the catalyst, bulk Aquivion presented more limited performances compared to Aq-TiO$_2$ with 30% and 40% of active phase on the composite. This behaviour could be attributed to the difference accessibility of the active phase, between the supported and unsupported catalysts. Indeed, the N$_2$ adsorption/desorption analyses showed that pure Aquivion is associated with very small surface areas, in the range of 0.2 – 0.3 m^2/g, while the Aq-TiO$_2$-30 and Aq-TiO$_2$-40 samples present higher values (Table 1). Clearly, the titania support provides porosity and surface area to the catalyst, which positively impact on the accessibility of the sulfonic active sites. Thus, even though the supported catalysts have a minor active phase content, the structure given by TiO$_2$ increase the mass transfer, and consequently, the catalytic activity. As a matter of fact, the presence of an inorganic component prevents the adhesion of Aquivion particles, increasing the number of accessible external sites. On the other hand, pure Aquivion presents a higher number of active sites, which, however, are poorly accessible and therefore lowers the observed activity. The application of an Aquivion/TiO$_2$ composite is also beneficial for compensating the tendency toward swelling typical of this type of resins, thanks to the rigid inorganic matrix provided by the oxide. Moreover, practical considerations based on the ease of the load and unload of the reactor need to be taken into account. With pure Aquivion, the reuse of catalyst shows some concerns due to the tendency of the material to swell and to adhere to the walls of the reactor.

Finally, the dilution of Aquivion with an inexpensive oxide reduces the high costs associated with this type of catalysts while increasing the productivity of the system. As a matter of fact, Fig. 11 displays the productivity in ethylene as a function of the actual Aquivion load on the TiO$_2$-based catalyst. For clarity, the sample name has been reported too, as can be found in Table 1. When pure Aquivion is used as catalyst, a minimum of productivity is observed. This is due to the mass transfer difficulties in the polymer and the inaccessibility of most of the active sites indeed, but also to the greater quantity of polymer needed when the
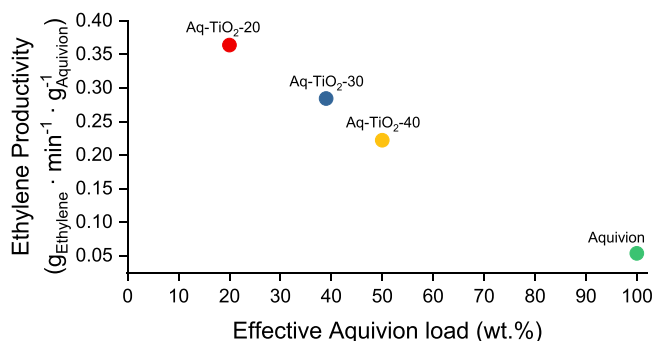
Fig. 11. Ethylene productivity as a function of the effective Aquivion load of Aquivion/TiO$_2$ composites and pure Aquivion.

catalyst is used in bulk. On the other hand, the three Aquivion/TiO$_2$ catalysts all show a higher ethylene productivity (between 0.36 [g$_{ethylene}$ • min^{-1} • (g$_{Aquivion}$)$^{-1}$] for Aq-TiO$_2$-20 and 0.22 [g$_{ethylene}$ • min^{-1} • (g$_{Aquivion}$)$^{-1}$] for Aq-TiO$_2$-40), which is attributable to the lower active phase load present in composite catalysts and to the higher catalytic activity reached. Based on these considerations, it appears once again that composite materials based on a perfluorosulphonic acid polymer, and an inorganic oxide present incontestable advantage compared to the use of the sole polymer.

Once the superiority of composite Aquivion/TiO$_2$ catalysts has been clarified, it is necessary to evaluate the influence that the synthetic method has on TiO$_2$-based catalysts. This has been done by comparing Aq-TiO$_2$-40 and Aq-TiO$_2$-40 W, both with 40 wt% of Aquivion and respectively synthesised with SFD and wet impregnation (Fig. 12). Analogously to what has been observed with SiO$_2$, the SFD method has been proved to produce catalysts with superior features compared to wet impregnation. Indeed, the EtOH conversion and ethylene selectivity values are complete for the SFD catalyst, while are slightly lower for the impregnated one (93% and 89% respectively). Moreover, no DEE production was observed with Aq-TiO$_2$-40, while its impregnated
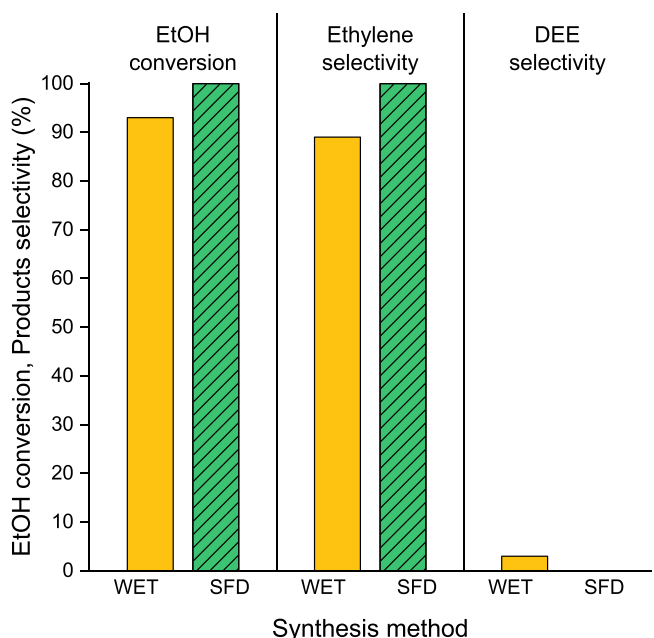
Fig. 12. The dependence of conversion and selectivity on the synthesis method (WET= wet impregnation, SFD= spray freeze drying) using Aquivion/TiO$_2$ catalysts with 40 wt% Aquivion load. Test conditions: T = 150 °C, τ = 1 s, EtOH = 1% v/v. Selectivity were not compared in condition of iso-conversion but in the same reaction conditions.

counterpart presents a 3% selectivity for this by-product.

The results obtained with SiO$_2$ and TiO$_2$-based catalysts confirm that SFD synthetic method has a positive contribution to the catalytic activity of Aquivion based catalysts, regardless from the type of support utilised.

Based on the complete conversion obtained with Aq-TiO$_2$-30 and its superior productivity (normalized considering the polymer loading) compared to Aq-TiO$_2$-40, the stability of this catalyst in the reaction conditions was investigated. Ethanol conversion and products selectivity were monitored during a 15-h test, performed at 130 °C (Fig. 13). The choice of a lower reaction temperature than the one used for the previous tests was justified by the extremely high conversion and selectivity values obtained with Aq-TiO$_2$-30 at 150 °C, which are not compatible with the requirements of stability evaluations. The catalyst performance appears to be stable with time on stream, and the material does not show any evident deactivation trend.

Finally, after all these considerations, the activity of Aq-TiO$_2$-30 has been assessed with various feeds. The EtOH volume percentage in the entering stream has been increased from 1% to 3% and 5%, and the effect on conversion and selectivity at 150 °C is reported in Fig. 14. The EtOH increase in the feed negatively impacts on its conversion, which diminishes from 100% (EtOH: 1% v/v) to 83% and 76% (EtOH: 3% and 5%). However, the major effect is observed over the products selectivity. Ethylene selectivity plummets from 100% to 19%, when EtOH concentration goes from 1% to 5%. Contrariwise, diethyl ether, which is not produced at the lower EtOH concentration, becomes the main product with the 3% and 5% EtOH feed, with a 62% and 80% selectivity, respectively. The trend of products selectivity goes accordingly to the considerations drawn by Alexopoulos et al. with their DFT studies about ethanol dehydration [45]. At low ethanol pressures, ethylene has been proved to be the favourable product. This is linked with the direct dehydration of ethanol, which follows a monomolecular reaction path and therefore is favoured at lower ethanol feed concentrations. On the other hand, high ethanol pressures favour the bimolecular condensation that leads to DEE. Thus, as the EtOH concentration increases, an increase in DEE selectivity is observed as well, while selectivity for ethylene experiences a drop.

4. Conclusions

Hybrid polymer/oxide composites (perfluorosulfonic superacid resin- Aquivion® PFSA with SiO$_2$ and TiO$_2$) were prepared with high surface area and homogeneous dispersion of different components through heterocoagulation and spray-freeze-drying of sols containing the precursor of the active phases. The hybrid materials were applied to the gas phase dehydration of ethanol to ethylene in mild conditions (150 −200 °C). Prepared catalysts with different amounts of components were active at low temperature and stable in the studied reaction conditions. The increase of porosity and the stability of the active sites improved the activity of these composites, compared to the pure Aquivion® PFSA, and allowed to reduce the amount of the superacid resin, increasing the productivity. The type of encapsulated oxide, TiO$_2$ or SiO$_2$, modified the performance of the catalysts. In particular, acid resin based on TiO$_2$ catalysts gave much higher conversion and selectivity in ethylene at very low temperature also respect to catalysts prepared by conventional impregnation methods with the same composition.

CRediT authorship contribution statement

Martina Battisti: Writing – review & editing. **Sara Andreoli:** General Investigation, Data curation, Writing – original draft. **Riccardo Bacile:** Specific investigation, Data curation. **Oldani Claudio**: Resources, Validation. **Simona Ortelli:** Specific investigation**,** Writing – review & editing. **Anna Luisa Costa:** Conceptualization, Methodology, Writing – review & editing. **Giuseppe Fornasari:** Supervision, Data curation, Writing – review & editing, Funding acquisition. **Stefania Albonetti:** Conceptualization, Methodology, Writing – review & editing,
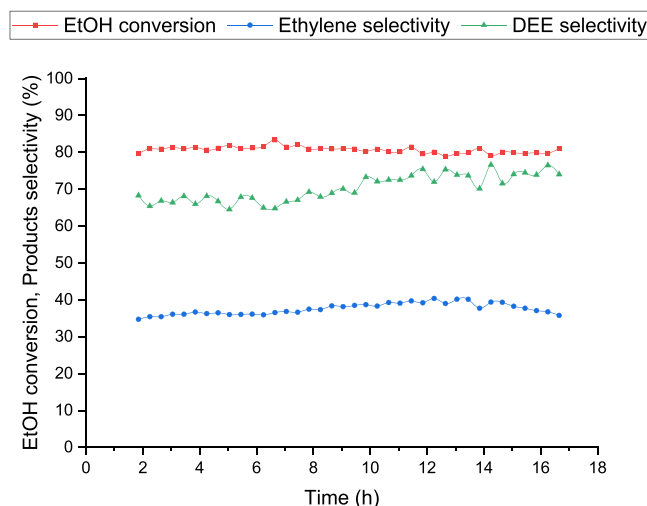

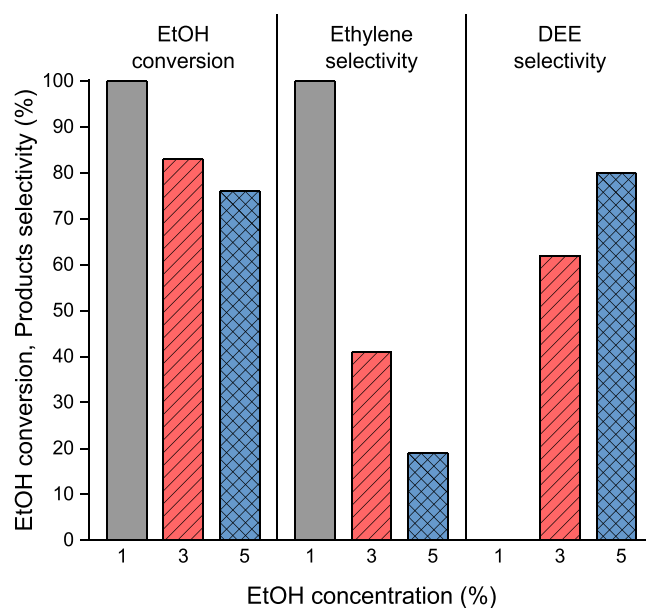**Fig. 13.** Durability test for Aq-TiO$_2$-30. Test conditions: T = 130 °C, τ = 1 s, EtOH = 1% v/v.

Fig. 14. Influence of the EtOH concentration in the feed (1, 3 or 5%) over conversion and selectivity for Aq-TiO$_2$-30. Test conditions: T = 150 °C, τ = 1 s.

Project administration.

Declaration of Competing Interest

The authors declare the following financial interests/personal relationships which may be considered as potential competing interests: Oldani Claudio reports financial support was provided by Solvay Specialty Polymers SpA.

Data Availability

Data will be made available on request.

Appendix A. Supporting information

Supplementary data associated with this article can be found in the online version at doi:10.1016/j.apcata.2023.119065.

References

[1] M. Frosi, A. Tripodi, F. Conte, G. Ramis, N. Mahinpey, I. Rossetti, J. Ind. Eng. Chem. 104 (2021) 272.

[2] M. Zhang, Y. Yu, Ind. Eng. Chem. Res. 52 (2013) 9505–9514.

[3] P. Bernardo, E. Drioli, Fuel Process. Technol. 212 (2021), 106624.

[4] S. Vaud, N. Pearcy, M. Hanževački, A.M.W. Van Hagen, S. Abdelrazig, L. Safo, M. Ehsaan, M. Jonczyk, T. Millat, S. Craig, E. Spence, J. Fothergill, R. R. Bommareddy, P.-Y. Colin, J. Twycross, P.A. Dalby, N.P. Minton, C.M. Jäger, D.-H. Kim, J. Yu, P.-C. Maness, S. Lynch, C.A. Eckert, A. Conradie, S.J. Bryan, Metab. Eng. 67 (2021) 308–320.

[5] W. Wu, H. Hu, D. Ding, Cell Reports Physical, Science 2 (12) (2021), 100405.

[6] M.H. Karimi Darvanjooghi, M. Malakootikhah, S. Magdouli, S.K. Brar, J. Membr. Sci. 643 (2022), 120044.

[7] D. Fan, D.-J. Dai, H.-S. Wu, Materials 6 (2013) 101–115.

[8] T.K. Phung, L. Proietti Hernández, A. Lagazzo, G. Busca, Appl. Catal. A: Gen. 493 (2015) 77–89.

[9] S.P. Banzaraktsaeva, E.V. Ovchinnikova, I.G. Danilova, V.V. Danilevich, V. A. Chumachenko, Chem, Eng. J. 374 (2019) 605–618.

[10] M.C.H. Clemente, G.A.V. Martins, E.F. de Freitas, J.A. Dias, S.C.L. Dias, Fuel 239 (2019) 491–501.

[11] R. Himmelmann, E. Klemm, M. Dyballa, Catal. Sc. Technol. 11 (2021) 3098–3107.

[12] D. Masih, S. Rohani, J.N. Kondo, T. Tatsumi, Microporous Nanoporous Mat. 282 (2019) 91–99.

[13] T. Kamsuwan, P. Praserthdam, B. Jongsomjit, Catal. Commun. 137 (6) (2020), 105941.

[14] M.A. Harmer, Q. Sun, Appl. Catal. A: Gen. 221 (2001) 45–62.

[15] N.V. Vlasenko, P.E. Strizhak, J. Appl. Polym. Sci. 51926 (2021) 1–20.

[16] W. Fang, S. Wang, A. Liebens, F. De Campo, H. Xu, W. Shen, M. Pera-Titus, J.-M. Clacens, Catal. Sci. Technol. 5 (8) (2015), 3980–90.

[17] A. Karam, K. De Oliveira Vigier, S. Marinkovic, B. Estrine, C. Oldani, F. Jérôme, ACS Catal. 7 (2017) 2990–2997.

[18] A. Karam, K. De Oliveira Vigier, S. Marinkovic, B. Estrine, C. Oldani, F. Jérôme, ChemSusChem 10 (2017) 3604–3610.

[19] Y. Wang, Y. Dou, H. Zhang, B. Gu, C. Oldani, Q. Tang, F. Jing, Q. Cao, W. Fang, Mol. Catal. 520 (2022) 112159–112166.

[20] H.G. Bernal, C. Oldani, T. Funaioli, A.M. Raspolli Galletti, N. J. Chem. 43 (37) (2019) 14694–14700.

[21] L. Bianchi, E. Ballerini, M. Curini, D. Lanari, A. Marocchi, C. Oldani, L. Vaccaro, ACS Sustainable, Chem. Eng. 3 (2015) 1873–1880.

[22] S. Andreoli, C. Oldani, V. Fiorini, S. Stagni, G. Fornasari, S. Albonetti, Appl. Catal. A: Gen. 597 (9) (2020), 117544.

[23] A. Karam, A. Franco, M. Limousin, S. Marinkovic, B. Estrine, C. Oldani, K. De Oliveira Vigier, R. Luque, F. Jérôme, Catal. Sci. Technol. 9 (2019) 1231–1237.

[24] N.V. Vlasenko, P.E. Stryzhak, Theoretical and Experimental, Chemistry 56 (5) (2020) 309–328.

[25] P.M. Forster, A.K. Cheetham, Top. Catal. 24 (1–4) (2003) 79–86.

[26] L. Degirmenci, N. Octar, G. Dogu, AIChE J. 57 (11) (2011) 3171–3181.

[27] M.E. Chimienti, L.R. Pizzio, C.V. Caceres, M.N. Blanco, Appl. Catal. A: Gen. 208 (2001) 7–19.

[28] A. Gil, L. Santamaria, S.A. Korill, M.A. Vicente, L.V. Barbosa, S.D. de Souza, L. Marcal, E.H. de Faria, K.J. Ciuffi, J. Environ. Chem. Eng. 9 (2021) 105808(18).

[29] V. Dufaud, M.E. Davis, J. Am. Chem. Soc. 125 (2003) 9403–9413.

[30] J.A. Melero, R. van Grieken, G. Morales, Chem. Rev. 106 (2006) 3790–3812.

[31] W. Long, C.W. Jones, A.C.S. Catal 1 (2011) 674–681.

[32] Y. Dou, M. Zhang, S. Zhou, C. Oldani, W. Fang, Q. Cao, Eur, J, Inorg. Chem. 33 (2018) 3706–3716.

[33] F.Y. Lu, H.Y. Fan, A. Stump, T.L. Ward, T. Rieker, C.J. Brinker, Nature 398 (1999) 223–226.

[34] D.P. Debecker, S. Le Bras, C. Boissiere, A. Chaumonoot, C. Sanchez, Chem. Soc. Rev. 47 (2018) 4112–4155.

[35] V. Smeets, W. Baaziz, O. Ersen, E. Gaigneaux, C. Boissiere, C. Sanchez, D. P. Debecker, Chem. Sci. 11 (2020) 954–961.

[36] C. Paris, A. Karelovic, R. Manrique, S. Le Bras, D.F. Devred, V. Vykoukal, A. Styskalik, P. Eloy, D.P. Debecker, ChemSusChem 13 (23) (2020) 6409–6417.

[37] M. Van der Verren, V. Smeets, A. vander Straeten, C. Dupont-Gillain, D. P. Debecker, Nanoscale Adv. 3 (6) (2021) 1646–1655.

[38] D.P. Debecker, V. Smeets, M. Van der Verren, H. Meerssman Arango, M. Kinnaer, F. Devred, Current Opinion in Green and Sustainable, Chemistry 28 (2021), 100437.

[39] H.M.J.M. Wedershoven, J.C.H. Zeegers, A.A. Darhuber, Chem. Eng. Sci. 181 (2018) 92–100.

[40] M. Blosi, A. Brigliadori, I. Zanoni, S. Ortelli, S. Albonetti, A.L. Costa, J. Environ. Manag. 304 (2022), 114187.

[41] A. Lolli, M. Blosi, S. Ortelli, A.L. Costa, I. Zanoni, D. Bonincontro, F. Carella, S. Albonetti, Catal. Today 334 (2019) 193–202.

[42] A. Allegri, V. Maslova, M. Blosi, A.L. Costa, S. Ortelli, F. Basile, S. Albonetti, Molecules 25 (20) (2020) 5225.

[43] ⟨https://www.chempoint.com/products/grace/ludox-monodispersed-collo idal-silica/ludox-colloidal-silica/ludox-hs-40#product-overview⟩.

[44] Spadaro L., Frusteri F., Di Blasi O., Bonura G., Mezzapica A., Troglia C., Ghielmi A., Fluoropolymer Composition, assigned to Solvay Solexis S.p.A, WO2008043804.

[45] S. Ortelli, A.L. Costa, Nano-Struct. Nano-Objects 13 (2018), 155–62.

[46] J.R. Martínez, S. Palomares-Sánchez, G. Ortega-Zarzosa, F. Ruiz, Y. Chumakov, Mater. Lett. 60 (29–30) (2006) 3526–3529.

[47] S. Musić, N. Filipović-Vincekovic, L. Sekovanić, Braz. J, Chem. Eng. 28 (1) (2011) 89–94.

[48] A. Rolfi, C. Oldani, L. Merlo, D. Facchi, R. Ruffo, J. Power Sources 396 (2018) 95–101.

[49] J. Chabé, M. Bardet, G. Gébel, Solid State Ion. 229 (2012) 20–25.

[50] J. Yu, H. Yu, B. Cheng, M. Zhou, X. Zhao, Journal of Molecular Catalysis A, Chemical 253 (2006) 112–118.

[51] K. Alexopoulos, M. John, K. Van der Borght, V. Galvita, M.-F. Reyniers, G.B. Marin, J. Catal. 339 (2016) 173–185.

[52] Y. Dou, S. Zhou, C. Oldani, W. Fang, Q. Cao, Fuel 214 (2018) 45–54.

[53] H. Knözinger, Angew Chem (Eds.), Int, 7, 1968, pp. 791–805.

[54] R. Bringue, J. Tejero, M. Iborra, J. Izquierdo, C. Fite, F. Cunill, Chem. Eng. J. 145 (1) (2008) 135–141.

[55] K. Liu, M. Cao, A. Fujishima, L. Jiang, Chem. Rev. 114 (19) (2014) 10044–10094.